Layer interface roughness effects in the coherent intraband transitions of excitons in quantum well structures

S. M. Sadeghi
The University of British Columbia, Department of Physics and Astronomy, 6224 Agricultural Road, Vancouver, B.C., Canada V6T 1Z1 and Department of Physics, University of Toronto, 60 St. George Street, Toronto, Ontario, Canada M5S 1A7

J. Meyer
The University of British Columbia, Department of Physics and Astronomy, 6224 Agricultural Road, Vancouver, B.C., Canada V6T 1Z1
(Received 12 January 2000)

Using photoluminescence spectroscopy we study the effects of exciton localization and interface growth islands in the coherent intraband transitions between the exciton states associated with the first and second conduction subbands. We show that the growth islands can act as submicron quantum systems with distinct energy-level configurations. Our results show that these systems interact differently with an intense infrared laser, causing a nearly two-dimensional medium with spatially modulated optical properties. We also show that the exciton localization enhances the coherent intraband transitions and discuss how these transitions can be used to study morphology of the interfaces between quantum well layers.

I. INTRODUCTION

Layer interface roughness, alloy fluctuations, impurities, etc., can strongly affect the optical and transport properties of quantum wells (QW's). Due to their statistical nature, these defects lead to potential fluctuations that are responsible for localization and dephasing of excitons.[1,2] The pertinent features of these effects in the photoluminescence (PL) spectra of QW's are Stokes shifts, inhomogeneous broadening, monolayer (ML) splitting, etc.[3,4] The potential fluctuations are also related to resonant Rayleigh scattering[5,6] and some other effects.[3]

While these defects have undesirable effects that may hinder the device application of QW's, they present new opportunities to study nonlinear optics of QW's with potentially new applications. The objective of this paper is to address this issue by studying the effects of the interface potential fluctuations in the coherent intraband transitions between excitons in QW's. These transitions are caused by exciting electrons from the exciton states associated with the first conduction subband ($E1$-$HH1$) to those associated with the second subband ($E2$-$HH1$). It has been shown that when these transitions are strongly driven by an infrared (IR) laser, the near band-edge absorption[7] and emission spectra[8] are modified strongly. In this paper we show how such transitions are affected by the localization of excitons (microroughness effects) and by the growth islands (macroroughness effects).

The results of this paper may shed some light on the optics of QW's. They show that the growth islands can act as submicron optical systems with distinct electronic and excitonic energy-level configurations. Therefore an IR laser with polarization along the growth direction can affect some of these systems strongly and leaves some other systems unchanged. Since this can lead to a nearly two-dimensional medium with spatially (laterally) modulated nonlinear optical properties, it may have some applications for optical and photonic devices. Our results also show that the coherent intraband transitions may be used as a tool to study the morphology of the interfaces between layers of QW's and to investigate the dephasing rates of excitons.

II. INTRABAND EXCITONIC COUPLING IN THE PRESENCE OF INTERFACE POTENTIAL FLUCTUATIONS

The scale of layer interface fluctuations plays a major role in the dynamics of excitons in QW's. When it is less than the exciton Bohr radius (microroughness), they can cause exciton localization, enhancement of the homogeneous and inhomogeneous broadening of the QW emission spectra, etc. In addition to microroughness, in structures prepared with growth interruption, although the layer interfaces are smoother, they may have large scale fluctuations or growth islands (macroroughness).[9] These islands can split the PL spectra of QW's, causing monolayer (ML) splitting peaks.[10] In addition to layer interface roughness, alloy fluctuations, impurities, etc., also contribute to the potential fluctuations experienced by excitons. A full quantitative treatment of these potential fluctuations is complicated. It requires detailed information about the statistical features of the interfaces and other imperfections. These features change not only from one sample to another, but also from one part of a sample to another. In addition to the complex statistical nature of the interface microroughness, one should also consider lateral shapes of the islands, correlations between sizes and shapes of adjacent islands, etc.[11,12] Therefore, for the benefit of focusing on our objectives in this paper, we treat the effects of the interface fluctuations in the evolution of the emission spectra of an infrared-coupled QW at a phenomenological level. Using this model we consistently describe our experimental results.

The $E1$-$HH1$ excitons are generated after momentum and energy relaxation of the photoexcited electrons in $E1$ and holes in $HH1$. In the presence of an IR laser near resonance with the transition between $E1$ and $E2$ and polarized

along the growth direction, the electrons are shared between the bound states of the excitons associated with these subbands.[13] The interaction term of this laser with the QW is given by

$$H_1 = -\sum_{n,n'} \mu_{12}^{snn'} \{E(t)|\Psi_{E2\text{-}HH1}^{n's}\rangle\langle\Psi_{E1\text{-}HH1}^{ns}| + E^*(t)|\Psi_{E1\text{-}HH1}^{ns}\rangle\langle\Psi_{E2\text{-}HH1}^{n's}|\}. \quad (1)$$

Here $\mu_{12}^{snn'}$ is the electric-dipole moment for the transitions between the excitons states $\Psi_{E1\text{-}HH1}^{ns}$ and $\Psi_{E2\text{-}HH1}^{n's}$. n and n' refer to the principle hydrogenlike quantum numbers. In Eq. (1) we ignore the nondiagonal transitions ($n \neq n'$), because these transitions are weaker than the diagonal ones ($n = n'$),[8] and the IR laser is considered to be nearly resonant with the diagonal transitions. Also since here the photoexcited carrier densities are low, we ignore the many-body effects and consider the emission spectra of the QW are mostly caused by the radiative decay of $\Psi_{E1\text{-}HH1}^{1s}$.[14] This means that the coupling processes are basically between excitons states with $n=1$. In Eq. (1) $E(t)=Ee^{-i\omega t}$ refers to the IR laser within rotating-wave approximation.

In addition to the IR laser, the photoexcited electrons and holes are affected by the potential fluctuations,

$$V_{\text{fluc}} = V_{\text{fluc}}^{\text{micro}} + V_{\text{fluc}}^{\text{macro}}. \quad (2)$$

Here $V_{\text{fluc}}^{\text{micro}}$ and $V_{\text{fluc}}^{\text{macro}}$ refer to the potential terms associated with the interface microroughness and growth islands, respectively. Adding these terms to the Hamiltonian of the system $H=H_0+H_1$, we can obtain the equations of the motion of the system using

$$\frac{\partial \rho^{1s}}{\partial t} = -\frac{i}{\hbar}[H + V_{\text{fluc}}, \rho^{1s}] + \lambda_{1s}. \quad (3)$$

H_0 is the Hamiltonian of the system in the absence of the infrared laser and λ_{1s} is the pump rate of the system caused by the visible laser. To treat Eq. (3) at our phenomenological level we introduce the effects of $V_{\text{fluc}}^{\text{macro}}$ by solving Eq. (3) for each growth island. For each island we then consider the effects of $V_{\text{fluc}}^{\text{micro}}$ by choosing the proper values of the binding energies and dephasing rates of excitons. These values are estimated based on the experimental or theoretical studies of others.[15,16] Based on these considerations the equations of motion for an island are obtained as follows:[17]

$$\left.\frac{d\rho_{11}^{1s}}{dt}\right|_{is} = \frac{1}{\tau_2^{1s}}\rho_{22}^{1s} + \frac{1}{\tau_3^{1s}}\rho_{33}^{1s} - \lambda_{1s}, \quad (4)$$

$$\left.\frac{d\rho_{22}^{1s}}{dt}\right|_{is} = -i\Omega(\rho_{32}^{1s} - \rho_{23}^{1s}) - \frac{1}{\tau_2^{1s}}\rho_{22}^{1s} + \lambda_{1s}', \quad (5)$$

$$\left.\frac{d\rho_{33}^{1s}}{dt}\right|_{is} = -i\Omega(\rho_{23}^{1s} - \rho_{32}^{1s}) - \frac{1}{\tau_3^{1s}}\rho_{33}^{1s} - \frac{1}{\tau_3^{1s\prime}}\rho_{33}^{1s}, \quad (6)$$

$$\left.\frac{d\rho_{21}^{1s}}{dt}\right|_{is} = \left(iE_{1s}^1 - \frac{1}{T_{12}^{1s}}\right)\rho_{21}^{1s} + i\Omega\rho_{31}^{1s}, \quad (7)$$

$$\left.\frac{d\rho_{31}^{1s}}{dt}\right|_{is} = \left[i(E_{1s}^2 - \hbar\omega) - \frac{1}{T_{13}^{1s}}\right]\rho_{31}^{1s} + i\Omega\rho_{21}^{1s}, \quad (8)$$

$$\left.\frac{d\rho_{23}^{1s}}{dt}\right|_{is} = \left(i\Delta - \frac{1}{T_{23}^{1s}}\right)\rho_{23}^{1s} + i\Omega(\rho_{33}^{1s} - \rho_{22}^{1s}). \quad (9)$$

Here ρ_{11}^{1s}, ρ_{22}^{1s}, and ρ_{33}^{1s} refer, respectively, to the probability of finding a hole in $HH1$ and an electron in $E1$ or $E2$ when they constitute the $\Psi_{E1\text{-}HH1}^{1s}$ and $\Psi_{E2\text{-}HH1}^{1s}$ excitons. Ω is the Rabi frequency of the IR field. Δ is the detuning of the IR field given by

$$\Delta = E_{1s}^2 - E_{1s}^1 - \hbar\omega. \quad (10)$$

Here E_{1s}^1 and E_{1s}^2 are the binding energies of the $\Psi_{E1\text{-}HH1}^{1s}$ and $\Psi_{E2\text{-}HH1}^{1s}$, respectively. These energies are renormalized by $V_{\text{fluc}}^{\text{micro}}$. They are also different from one island to another, as will be discussed in the following.

τ_2^{1s} in Eq. (5) represents the intrinsic radiative recombination time of the bound $\Psi_{E1\text{-}HH1}^{1s}$ excitons. It is estimated to be around 25 ps.[18] Since the QW is symmetric the radiative decay rate of the $E2$-$HH1$ is zero ($1/\tau_3^{1s}=0$). $1/\tau_3^{1s\prime}$, is the nonradiative decay rate of such excitons, which is caused by their LO-phonon emission. This process generates electrons with relatively large wave vectors in $E1$ and holes at the top of the valence subband ($HH1$). As a result, $1/\tau_3^{1s\prime}$, contributes to the ''recycling'' and loss rates of the electron-hole pairs. The ''recycling'' rate occurs via energy relaxation of electrons after they undergo intersubband transitions. When they reach the bottom of $E1$ they reconstitute radiative bound states with holes ($E1$-$HH1$ excitons). Note that the energy relaxation of electrons in $E1$ is very fast. However, when they bind with holes and form bound excitons, their energy and momentum relaxation take a relatively long time.[19] The ''recycling'' rate and that caused by the direct excitation of electrons into $E1$ by the visible laser are presented by λ_{1s}' in Eq. (5). The loss rate represents the rate at which the electron-hole pairs recombine nonradiatively. As will be shown in the following, this rate can lead to strong quenching of the emission spectra of the $E1$-$HH1$ excitons, depending on the infrared frequency and intensity. $1/T_{ij}^{1s}$ are the polarization dephasing rates consisting of the energy relaxation rates of the electrons and holes and elastic scattering rates of excitons with the potential fluctuations.

In the following we use this model to analyze our experimental results and predict some other effects. To do this we solve Eqs. (4)–(9) in steady state. This is because the width of the IR laser pulses is considered to be much larger than the characteristic dephasing time of the excitons. Having the density matrix we find the emission spectra of the QW using linear-response theory.

III. EFFECTS OF LOCALIZATION IN THE INTRABAND TRANSITIONS OF EXCITONS

In this section we study the effects of the exciton localization caused by the interface roughness in the intraband coupling of QW's. The details of the sample has been reported elsewhere.[8] It contained fifty 7.3 nm undoped wells (GaAs) sandwiched between 18.1 nm barriers

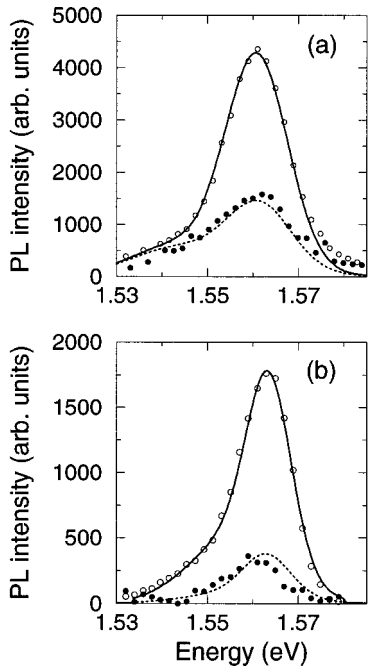

FIG. 1. PL spectra of the QW in the absence (open circles) and presence (dots) of a CO_2 laser with ~ 1 MW/cm^2 intensity and (a) 121- and (b) 118-meV photon energies. Sample temperatures at (a) and (b) are 77 and 10 K, respectively.

($Al_{0.28}Ga_{0.72}As$). We used a hybrid CO_2 laser with a 500 ns pulse width and ~ 1 MW/cm^2 intensity to couple the $E1$-$HH1$ and $E2$-$HH1$ excitons. To pump the QW, a frequency doubled Nd:YAG (yttrium aluminum garnet) laser with 2.34-eV photon energy and 70-ps pulse width was used. This laser was focused at the surface of the QW within the area affected by the CO_2 laser.

Since localization of excitons depends strongly on the sample temperature, we studied the IR coupling process at 10 and 77 K. At 10 K, localization of excitons is dominant and at 77 K most of them are thermally free. The transition energies at 10 and 77 K were estimated to be ~ 119 and ~ 121 meV, respectively. At each temperature we tuned the CO_2 laser to become near resonance with the transitions between $1s$ states of the $E1$-$HH1$ and $E2$-$HH1$ excitons.

Figure 1 shows the evolution of the emission spectra of the QW at (a) 77 K and (b) 10 K. Although the CO_2 intensity was the same for both cases the spectrum at 10 K with $\Delta \sim 1$ meV is quenched more than that at 77 K with $\Delta \sim 0$ [Fig. 1(b)]. This can be associated with the fact that as the sample temperature decreases excitons become more localized or spend more time in the bound states associated with the potential fluctuations. Therefore, in contrast to free excitons, they do not have efficient scattering with acoustic phonons and the potential fluctuations. This decreases their dephasing rates, making the IR coupling between $E1$-$HH1$ and $E2$-$HH1$ excitons more efficient. As mentioned before, since the $E2$-$HH1$ excitons decay by emitting LO-phonons, they are disintegrated into electrons with large wave vectors in $E1$ and holes at the top of $HH1$. As a result the IR coupling of the $E1$-$HH1$ and $E2$-$HH1$ excitons increases the chance of the nonradiative recombination of the electrons and holes and significantly quenches the PL spectra. The slight redshift in Fig. 1(b) is the result of small detuning of the CO_2 laser from the transition between the $E1$-$HH1$ and $E2$-$HH1$ excitons (~ 1 meV).

To discuss these results in a semiquantitative fashion we apply our model to the systems of Figs. 1(a) and 1(b). For the case of 10 K [Fig. 1(b)], the average width of the localized excitons ($2/T_{12}^{1s}$) in the tail is considered to be 0.15 meV (deep bound states) and in the main peak equals 0.5 meV (partially localized excitons). For the case of 77 K we assumed $2/T_{12}^{1s} \sim 0.4$ meV in the tail, and $2/T_{12}^{1s} \sim 1$ meV in the main peak. Also because of the fast decay of the $E2$-$HH1$ excitons in both cases we consider $2/T_{13}^{1s} = 5$ meV. The results of calculations in the absence (solid line) and presence (dotted line) of the CO_2 laser are shown in Fig. 1. Each solid line is obtained by fitting the uncoupled emission spectrum (circles) with two Gaussian distributions of excitons, one for the tail and one for the main peak. In the presence of the CO_2 laser the fitting parameter for matching between the model and experiment was the effective nonradiative decay rate of the $E1$-$HH1$ excitons or the loss rate. In the case of Fig. 1(a) [Fig. 1(b)] a reasonable match was obtained considering this rate equal to 0.15 (0.3) ps^{-1}. The reason that at 77 K the loss rate is smaller than that at 10 K, can be related to the higher mobility of the photoexcited electrons and holes at 77 K.[20] The slight discrepancy between the theory and experiment can mainly be related to the detailed statistical nature of the layer interfaces that has not been included in our model.

IV. GROWTH ISLAND EFFECTS IN THE INTRABAND COUPLING OF EXCITONS

As mentioned before when a sample is prepared with growth interruption the layer interfaces may contain growth islands.[9] Since the thickness of these islands may differ by one or more ML's, in narrow QW's they can lead to ML splitting peaks. These peaks are associated with the radiative decay of excitons localized in each island.[21] In this section we discuss the effects of these islands in the coherent intraband transitions between excitons. To do this we apply our model to a growth interrupted QW structure studied in Ref. 10. This structure consisted of five single GaAs wells separated by thick $Al_{0.4}Ga_{0.6}As$ barriers. The nominal widths of these wells were 3, 6, 11, 19, and 25 ML's.

The PL spectroscopy of this structure at 4.3 K has shown that the emission spectrum associated with the well with 19 ML's nominal width, contained three distinct ML splitting peaks and a small bump.[10] The peaks that occurred at ~ 1.582 (B), ~ 1.586 (C), and ~ 1.590 eV (D) could be associated with the growth islands with 20, 19, and 18 ML's, respectively. The bump (A) happened at ~ 1.579 eV and might be caused by islands with 21 ML's. The solid lines in Fig. 2 show the result of our calculations for the emission spectrum of this well in the absence of the infrared field. This spectrum is the result of overlap between four Gaussian emission spectra associated with excitons trapped in the four growth islands. Each Gaussian spectrum contains a large number of homogeneously broadened $E1$-$HH1$ excitons with ~ 0.15 meV linewidth ($2/T_{12}$). To study the evolution of this system in the presence of a laser responsible for the intraband excitonic transitions, we consider the nonradiative decay rate of excitons 0.3 ps^{-1}, similar to that estimated in the preceding section. Also the $E2$-$HH1$ width is assumed

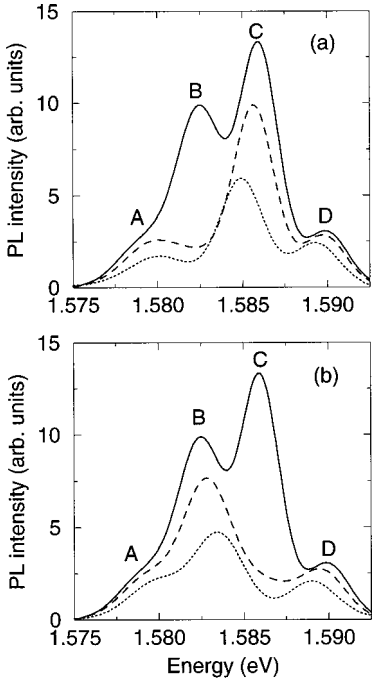

FIG. 2. Solid lines represent the emission spectrum of a QW with 19 ML's nominal width and four types of growth islands (similar to that reported in Ref. 10). The dashed and dotted lines show the evolution of the spectrum in the presence of an IR laser with $\Omega = 2.5$ and 5 ps^{-1}, respectively. The photon energies of the IR laser are 186 (a), and 195 (b) meV.

to be 5 meV$(2/T_{13})$. Figure 2 shows the results of the calculation when the infrared laser has (a) 186-or (b) 195-meV photon energies. Inspection of these results shows:

(i) When the intensity of the IR laser is $\sim 0.4\,MW/cm^2(\Omega = 2.5\,ps^{-1})$ and its photon energies 186 meV, as Fig. 2(a) shows (dashed line) the peak (B) is quenched such that it virtually vanishes. The bump (A) is resolved, and the peaks (D) and (C) are also quenched to some extent. When the intensity increases to about $1.5\,MW/cm^2(\Omega = 5\,ps^{-1})$ the whole spectrum is affected significantly (dotted line). Similar dynamics also occur when the IR laser photon energies are 195 meV [Fig. 2(b)]. Here, however, the peak (C) is quenched the most.

(ii) In addition to quenching, the ML splitting peaks are red or blueshifted. In the case of 186-meV photon energies [Fig. 2(a)] the peaks (C) and (D) are redshifted and the bump (A) is blueshifted. In the case of 195-meV photon energy [Fig. 2(b)], however, the peaks (D) and (B) are redshifted and blueshifted, respectively.

To analyze these results note that as mentioned before, the spectra in Fig. 2 are associated with the emission of the $E1$-$HH1$ excitons localized by the interface microroughness in the 18-, 19-, 20-, and 21-ML growth islands. The estimated energy spacing between $E1$-$HH1$ and $E2$-$HH1$ in these islands are, respectively, 205, 195, 186, and 176 meV. Therefore, when the infrared laser has 186-or 195-meV photon energies, it is detuned differently from the transitions between $E1$-$HH1$ and $E2$-$HH1$ excitons in these islands. As shown schematically in Fig. 3, when the IR photon energy is 186 meV this laser is resonant with the transition between the $E1$-$HH1$ and $E2$-$HH1$ excitons in the 20-ML

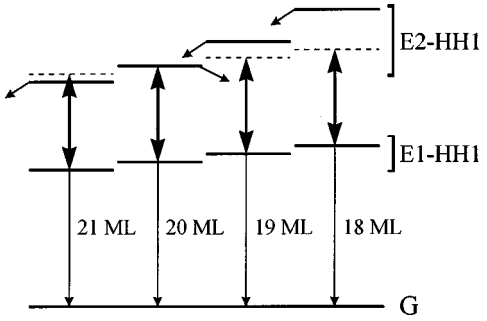

FIG. 3. Schematic diagrams of the IR coupling processes in the 21-, 20-, 19-, and 18-ML systems associated, respectively, with (A), (B), (C), and (D) in Fig. 2. In each ML system the lower and upper levels refer to the 1s states of the $E1$-$HH1$ and $E2$-$HH1$ excitons, respectively. The two-headed arrows refer to the IR laser coupling, the vertical downwards arrows to the radiative decay of the excitons, and the inclined arrows to the nonradiative LO-phonon decay processes of the $E2$-$HH1$ excitons.

system and detuned from the corresponding transitions in the 21-, 19-, and 18-ML systems by about -10, 9, and 19 meV, respectively. As a result, the 20-ML system is affected by the infrared laser significantly. This decreases the contribution of this system in the emission spectrum drastically, causing suppression of the peak (B). In addition to the quenching due to the detuned coupling processes of the 21-, 19-, and 18-ML islands, their emission peaks undergo redshifting or blueshifting. These are Stark shifts caused by the coherent mixing of the $E1$-$HH1$ and $E2$-$HH1$ excitons. When $\Delta < 0$ (21-ML system) we have blueshifting and for $\Delta > 0$ (19- and 18-ML systems) the emission peaks are redshifted. The dynamics of Fig. 2(b) are similar to those of Fig. 2(a). Here, however, the laser is resonant with the transitions between the 1s states of the $E1$-$HH1$ and $E2$-$HH1$ excitons in the 19-ML island.

The dynamics seen in Fig. 2 show that in narrow QW's the growth islands can act as submicron quantum systems with different electronic and excitonic energy configurations. Therefore, in the presence of an intense IR laser, while some of these systems are not affected significantly, some others undergo strong nonlinear regime. This leads to a spatially (laterally) inhomogeneous optical medium. Since one can design QW structures with peculiar nonlinear optical properties and can texture the interfaces with desired forms and dimensions, these results may have applications for new optical and photonic devices.

V. INTRABAND EXCITONIC TRANSITIONS AND MORPHOLOGY OF QW LAYER INTERFACES

In the previous sections we showed that the coherent intraband transitions between excitons in QW's depend strongly on layer interface fluctuations. This suggests that these transitions can be used to study the morphology of the interfaces between QW layers. Our objective in this section is to illustrate an application of this technique. To do this we studied the emission spectra of several lateral locations of our sample in the presence of a single mode CO_2 laser with 117-meV photon energy and ~ 1 MW/cm^2 intensity. Similar to Sec. III, this laser was p polarized and the photoexcited

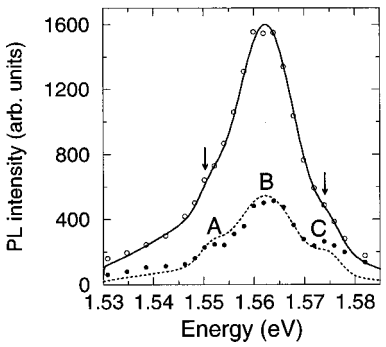

FIG. 4. PL emission spectra of the sample at a location different from that in Fig. 1(b). The dots present the emission spectrum in the presence of the CO_2 laser with the same intensity as that in Fig. 1(b) but with 117-meV photon energies. The solid and dashed lines refer to the theoretical results.

densities were kept low to ignore the carrier-carrier and carrier-exciton scattering processes. The sample temperature was 10 K.

As Fig. 4 shows, the PL spectrum from one of these locations (open circles) in the absence of the CO_2 laser, consists of one main peak and two bumps (arrows). In the presence of this laser, in addition to an extensive amount of quenching, the spectrum splits into a triplet (filled circles). The energy separations between the sideband peaks (A and C) and the central peak (B) are similar to those between the bumps (arrows) and the main peak. When we detected another location of the sample at the vicinity of that in Fig. 4, the emission spectrum became different. As Fig. 5 shows, here in the absence of the IR field, the spectrum contains a small peak at $\sim$20 meV below the main peak. In the presence of the CO_2 laser the whole spectrum undergo an immense quenching, but the lower-energy peak becomes more distinct.

Fig. 6 shows the emission spectra of the QW at the third location of the sample. Here the overall shape of the uncoupled PL spectrum is similar to those in Figs. 4 and 5. However, no imperfections such as those shown by arrows in Fig. 4 can be seen in Fig. 6. Also in contrast to Fig. 4 where the CO_2 laser split the spectrum into three peaks, here the spectrum becomes slightly redshifted.

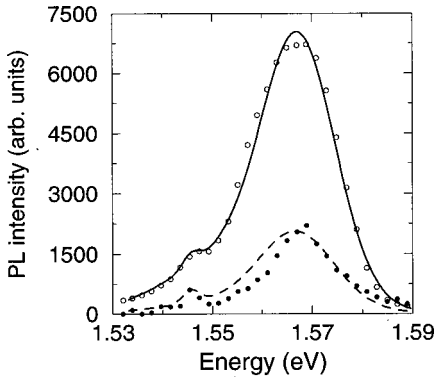

FIG. 5. PL emission spectra from a location of the sample at the vicinity of that in Fig. 4 in the absence (open circles) and presence (dots) of the CO_2 laser. Other specifications are the same as those in Fig. 4.

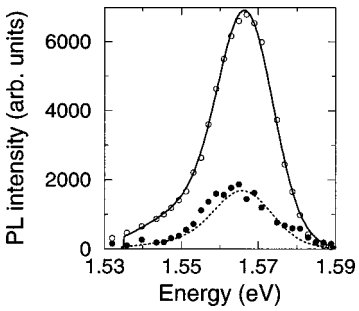

FIG. 6. PL emission spectra from a third lateral location of the sample. Other specifications are the same as those in Fig. 4.

The dynamics in Figs. 4–6 show how the coherent intraband transitions between excitons are sensitive to the layer interface morphology of the sample. In the case of the Fig. 6, the dynamics are very similar to those discussed in Sec. III [Fig. 1(b)]. However, since here the IR field detuning is larger than that in Fig. 1(b) ($\Delta \sim 2$ meV) the amount of the quenching is less and the spectrum is slightly more redshifted.

The dynamics in Figs. 4–5 provide some clues about some large scale interface defects. They show some similarities with those in Sec. IV where a single mode laser quenched ML splitting peaks of a growth interrupted QW. To speculate further, note that the large widths of the emission spectra in Figs. 4–5 are signs of rough interfaces. Therefore, one can expect some of the large scale defects act as ''effective growth islands.'' The features seen in Figs. 4–5 can be explained if we attribute them to these islands. To do this, note that in the absence of the CO_2 laser the emission spectra in Figs. 4 and 6 are similar if we ignore the bumps (arrows). This means that the main emission in Fig. 4 is associated with the nominal width of the QW (7.3 nm or $\sim$26 ML's) as one expects. On the other hand, since the energy spacings between the main peak and the bumps are $\sim$10 meV, the latter can be related to ''effective growth islands'' with $\sim$23 and $\sim$29 ML's. This leads us to a picture similar to that presented in Fig. 2, except for the transition energies between the $1s$ states of the $E1$-$HH1$ and $E2$-$HH1$ excitons. Here these energies are estimated to be 136, 119, and 103 meV in the 23-, 26-, and 29-ML systems, respectively. Therefore a CO_2 laser with 117-meV photon energies is, respectively, detuned by about 19, 2, and -14 meV from these transitions. For the system of Fig. 5, in addition to the dominant 26-ML system, we may consider small defects associated with 33 ML's.

The solid line in Fig. 4 shows the result of the theoretical fit to the emission spectrum in the absence of the laser field. This fit was obtained considering a spectrum similar to that in Fig. 6 (26-ML system contribution) and two Gaussian distributions associated with the 23 and 29-ML systems at ± 10 meV from the main peak. In the presence of the CO_2 laser a good match between the experiment and theory was reached (Fig. 4, dashed line) assuming the nonradiative decay rate of excitons equal to that obtained in Sec. III (0.3 ps^{-1}). The overall quenching here is the result of the effective transfer of excitons in the 26-ML system from the radiative states of the $E1$-$HH1$ excitons into the nonradiative states of the $E2$-$HH1$ excitons by the CO_2 laser. Since the 23- and 29-ML systems are virtually not effected by this

laser, their emission contributions are not changed significantly. Therefore, their relative emission shares with the whole spectrum increase, generating a triplet spectrum as that shown in Fig. 4. Similarly in the case of Fig. 5, the 33-ML systems are virtually left unaffected by the CO_2 laser. The solid and dashed lines here show the results of the model in the absence and presence of this laser using the same parameters as those of Fig. 4.

VI. CONCLUSIONS

In conclusion, we studied the effects of the layer interface roughness in the IR coherent coupling of excitons in QW's. We showed that localization of excitons enhances the coherent intraband transitions between the $E1$-$HH1$ and $E2$-$HH1$ excitons. It was also shown that these transitions were influenced by the growth islands differently, depending on their thickness.

ACKNOWLEDGMENTS

We are very grateful to T. Tiedje and M. Beaudoin for providing us with the sample. This research was supported by the Natural Sciences and Engineering Research Council of Canada.

[1] J. Hargarty, M. D. Sturge, C. Weisbuch, A. C. Gossard, and W. Wiegmann, Phys. Rev. Lett. **49**, 930 (1982).
[2] H. Hillmer, A. Forchel, R. Sauer, and C. W. Tu, Phys. Rev. B **42**, 3220 (1990).
[3] L. C. Andreani, G. Panzarini, A. V. Kavokin, and M. R. Vladimirova, Phys. Rev. B **57**, 4670 (1998).
[4] M. Gurioli *et al.*, Phys. Rev. B **44**, 3115 (1991); M. Ramsteiner, R. Hey, R. Klann, U. Jahn, I. Gorbunova, and K. H. Ploog, *ibid.* **55**, 5239 (1997).
[5] H. Stolz, D. Schrarze, W. von der Osten, and G. Wiemann, Phys. Rev. B **47**, 9669 (1993).
[6] V. I. Belitsky, A. Cantarero, S. T. Pavlov, M. Gurioli, F. Bogani, A. Vinattieri, and M. Colocci, Phys. Rev. B **52**, 16 665 (1995).
[7] D. Frohlich, Ch. Neumann, S. Spitzer, B. Uebbing, and R. Zimmermann, *Meeting on Optics of Excitons in Confined Systems, Giardini Naxos, 1991*, edited by A. D'Andrea, R. Del Sole, R. Girlanda, and A. Quatropani (Galliard, Great Yarmouth, Norfolk, 1991), p. 227.
[8] S. M. Sadeghi, J. Meyer, T. Tiedje, and M. Beaudoin (unpublished).
[9] R. Grousson, V. Voliotis, N. Grandjean, J. Massies, M. Leroux, and C. Deparis, Phys. Rev. B **55**, 5253 (1997).
[10] Mee-Koy Chin and C-P Luo, J. Lumin. **79**, 233 (1998).
[11] F. Große and R. Zimmermann, Superlattices Microstruct. **17**, 4399 (1995).
[12] C. Metzer, G. H. Dohler, and H. Sakaki, Phys. Status Solidi A **164**, 471 (1997); D. S. Citrin, Phys. Rev. B **47**, 3832 (1993).
[13] We assume in this paper that the transition energy between $E1$ and $E2$ is the same as that between $1s$ states of $E1$-$HH1$ and $E2$-$HH1$. For experimental evidence see P. Vagos, *et al.* in Phys. Rev. Lett. **70**, 1018 (1993).
[14] Note that our assumption that the emission spectra are caused by populating the exciton states may not be valid at high-carrier densities, see M. Kira *et al.*, Phys. Rev. Lett. **81**, 3263 (1998).
[15] U. Jahn, S. H. Kwock, M. Ramsteiner, R. Hey, H. T. Grahn, and E. Runge, Phys. Rev. B **54**, 2733 (1996).
[16] T. Takagahara, Phys. Rev. B **57**, 4670 (1998).
[17] A detailed discussion of these equations has been reported in S. M. Sadeghi and J. Meyer, J. Phys.: Condens. Matter **9**, 7685 (1997).
[18] L. C. Andreani, Solid State Commun. **77**, 641 (1991).
[19] T. C. Damen, J. Shah, D. Y. Oberli, D. S. Chemla, J. E. Cunningham, and J. M. Kuo, Phys. Rev. B **42**, 7434 (1990).
[20] Note that this phenomenon competes with the fact that as sample temperature increases the radiative decay of excitons decreases.
[21] K. Fujiwara, H. Katahama, K. Kanamoto, R. Cingolani, and K. Ploog, Phys. Rev. B **43**, 13 978 (1991).